Inonotus obliquus Protects against Oxidative Stress-Induced Apoptosis and Premature Senescence

Jong Seok Yun, Jung Woon Pahk, Jong Seok Lee, Won Cheol Shin, Shin Young Lee, and Eock Kee Hong*

In this study, we investigated the cytoprotective effects of *Inonotus obliquus* against oxidative stress-induced apoptosis and premature senescence. Pretreatment with *I. obliquus* scavenged intracellular ROS and prevented lipid peroxidation in hydrogen peroxide-treated human fibroblasts. As a result, *I. obliquus* exerted protective effects against hydrogen peroxide-induced apoptosis and premature senescence in human fibroblasts. In addition, *I. obliquus* suppressed UV-induced morphologic skin changes, such as skin thickening and wrinkle formation, in hairless mice *in vivo* and increased collagen synthesis through inhibition of MMP-1 and MMP-9 activities in hydrogen peroxide-treated human fibroblasts. Taken together, these results demonstrate that *I. obliquus* can prevent the aging process by attenuating oxidative stress in a model of stress-induced premature senescence.

INTRODUCTION

Reactive oxygen species (ROS), which are constantly produced in biological tissues, play significant roles in various cellular signaling pathways. Homeostasis between oxidants and antioxidants is necessary to minimize molecular, cellular and tissue damage. However, upsetting the balance in favor of oxidants results in oxidative stress and eventually oxidative damage (Rhee, 2006). The free radical theory of aging provides much support for ROS, such as superoxide, hydrogen peroxide and hydroxyl radicals, playing a role in the initiation and progression of the aging process (Harman, 1956). As evidence, aged animals have been shown to produce higher levels of ROS compared to younger animals. In addition, increased oxidative damage of DNA, proteins and lipids has been reported in aged animals (Chen, 2000).

Direct exposure of various cell types to oxidants such as hydrogen peroxide or ultraviolet (UV) radiation can directly induce apoptosis (Nobel et al., 1995). Enhanced apoptosis and elevated levels of ROS play a major role in aging (Schindowski et al., 2001). Apoptosis, or programmed cell death, is an important physiological process and occurs during tissue remodeling. Cells undergoing apoptosis show a sequence of cardinal morphological features, including membrane blebbing, cellular shrinkage and condensation of chromatin (Saraste and Pulkki, 2000). The mitochondria-mediated pathway, when stimulated, leads to the release of cytochrome c from the mitochondria and to the activation of the death signal (Scorrano, 2009; Yu et al., 2010). Apoptotic signaling and execution through this pathway depends on caspases, or aspartate-specific cysteine proteases, which are the key effector molecules in the apoptotic process (Cohen, 1997).

Oxidative stress has been shown to induce stress-induced premature senescence in fibroblasts (Dasari et al., 2006; Frippiat et al., 2001). Stress-induced premature senescence was recently invoked as an explanation of irreversible growth arrest characterized by senescence-specific cell morphology and gene expression, similar to the phenomenon of replicative senescence (Touissant et al., 2000). The number of senescence-associated β-galactosidase (SA-β-gal)-positive cells increases in older animals, and oxidative stress can be increased SA-β-gal activity *in vivo* (Serrano and Blasco, 2001). These data support stress-induced premature senescence models as representative tools for the investigation of aging.

Data on extracts isolated from *Inonotus obliquus* is highly impressive, and these extracts show promise for use as pharmacological therapeutics (Kim et al., 2006; 2007; Nakajima et al., 2009). However, the preventive effects of *I. obliquus* extracts on oxidative stress-induced apoptosis and premature senescence have never been investigated.

In the present study, we investigated the protective effects of *I. obliquus* on fibroblast senescence and apoptosis induced by oxidative stress, as well as the underlying mechanism of cytoprotection.

MATERIALS AND METHODS

Materials
Fetal bovine serum, penicillin G, streptomycin, and Dulbecco's modified Eagle's medium (DMEM) were obtained from GIBCO

Department of Bioengineering and Technology, Kangwon National University, Chuncheon 200-701, Korea
*Correspondence: ekhong@kangwon.ac.kr

Springer

(USA). Hydrogen peroxide, 3-(4,5-dimethylthiazol-2-yl)-2,5-diphenyltetrazolium bromide (MTT), gelatin, and β-casein were purchased from Sigma Chemical Co. (USA). Dichlorodihydrofluorescein diacetate (H$_2$DCFDA) was purchased from Molecular Probes (USA). All other chemicals were of Sigma grade. Antibodies to β-actin, pro-caspase 3, cleaved caspase 3, Bax, Bcl-2, horseradish peroxidase (HRP)-linked anti-rabbit IgG, and HRP-linked goat anti-mouse IgG were obtained from Cell Signaling (USA) and Santa Cruz Biotechnology (USA).

Sample and sample preparation
Dried fruiting bodies of *I. obliquus* were purchased from ChagaIn (Korea) and ground in a blender. A milled mushroom (20 g) was extracted with 10 volumes of distilled water at 80°C for 4 h. Extracts were centrifuged at 10,000 × g for 20 min, filtered through 0.45 μm Whatman filter paper to remove insoluble matter, and then lyophilized. Lyophilized *I. obliquus* extracts were prepared aseptically and kept in a refrigerator until use.

Animals and cell culture
Female SKH-1 hairless mice, 6 weeks old, were purchased from Charles River Orient Experimental Animal Breeding Center (Korea). The mice were maintained under constant conditions, i.e., 20-22°C ambient temperature, relative humidity of 50 ± 5%, 12/12 h light-dark cycle with free access to standard commercial diet and water. Human dermal fibroblasts were provided by Professor Y.H. Kang (Hallym University, Korea). Human dermal fibroblasts were cultured in DMEM medium supplemented with 10% heat inactivated fetal bovine serum, 2 mM glutamine, 100 U/ml penicillin and 100 μg/ml streptomycin. Cells were maintained at 37°C in a 5% CO$_2$ incubator. For this study, the cells used were early passages from 4 to 10.

Intracellular reactive oxygen species scavenging activity
To investigate the effect of *I. obliquus* extracts on oxidative stress, human dermal fibroblasts (2.5 × 10^4 cells/ml) were seeded in 12-well plates and incubated at 37°C to allow for cell attachment. After 48 h, the cells were treated with or without *I. obliquus* extracts for 4 h and then 1 mM hydrogen peroxide was added to each well of the plate. After 2 h, a 5 μM H$_2$DCFDA solution in PBS was added and the fluorescence was measured at an excitation and emission wavelength of 485 nm and 535 nm, respectively, by a microplate spectrofluorometer. For image analysis of intracellular ROS production, human dermal fibroblasts (2.5 × 10^4 cells/ml) were seeded in coverslip loaded 6-well plates and treated in the same manner as above. A H$_2$DCFDA solution was then added and incubated with the cells for 2 h at 37°C. Cells were then fixed with 3.7% paraformaldehyde for 20 min and washed with PBS. After washing with PBS, cells were mounted under glass coverslips with Vectashield (Brunschwig, The Netherlands) and observed. Photographs were taken under a fluorescence microscope (Jang et al., 2010).

Lipid peroxidation inhibitory activity
Lipid peroxidation was assayed by thiobarbituric acid (TBA) reaction (Jeong et al., 2009). In brief, human dermal fibroblasts were challenged with 1 mM hydrogen peroxide in the presence or absence of *I. obliquus* extracts, and the mixture was incubated for 2 h. The cells were then washed with PBS, harvested and homogenized in ice-cold 1.15% KCl. The homogenized cells were mixed with 8.1% sodium dodecyl sulfate, 20% acetic acid (pH 3.6) and 0.8% TBA, after which the mixture was heated to 95°C for 1 h. After cooling at room temperature, an n-butanol/pyridine mixture (15:1, v/v) was added, shaken thoroughly for 5 min and centrifuged at 1,000 × g for 10 min. The supernatant was isolated and the absorbance was determined at 535 nm.

Cell viability
The protective effects of *I. obliquus* extracts on the viability of hydrogen peroxide treated human dermal fibroblasts was measured using the MTT assay, which relies on the ability of viable cells to metabolically reduce the tetrazolium salt MTT to a purple formazan product, which can be quantified colorimetrically (Lee et al., 2009). Briefly, cell suspensions (2.5 × 10^4 cells/ml) were seeded in 96-well plates and incubated at 37°C to allow for cell attachment. After 48 h, the cells were treated with serum-free medium containing the indicated additives. At the end of each exposure time, 50 μl of the MTT stock solution (5 mg/ml) in serum-free medium were added to each well to reach a total reaction volume of 200 μl. After incubation for 2 h at 37°C, the supernatants were aspirated. The formazan crystal in each well was dissolved in isopropyl alcohol, and the absorbance was determined at 570 nm.

Flow cytometric analysis
Apoptosis-mediated cell death of human dermal fibroblasts was examined using a FITC-labeled annexin V/propidium iodide (PI) apoptosis detection kit (Molecular Probes, USA) according to the manufacturer's instructions. Briefly, cells were harvested by trypsinization, washed with PBS and centrifuged to collect the cell pellet. The number of cells was adjusted to 1 × 10^6 cells/ml. Cells were then resuspended in binding buffer (10 mM HEPES, 140 mM NaCl, 2.5 mM CaCl$_2$, pH 7.4) and then stained with FITC-labeled annexin V and PI at room temperature for 15 min in the dark. Flow cytometric analysis was performed using a FACSCalibur flow cytometer (Becton Dickinson, USA) within 1 h after supravital staining. FITC-labeled annexin V was analyzed using excitation and emission setting of 488 nm and 535 nm. PI was analyzed using excitation and emission setting of 488 nm and 575 nm. For each flow cytometer run, 10,000 cells were required. The percentages of cells were calculated by Cell Quest software (Becton Dickinson). The cells in the early stages of apoptosis were annexin V positive and PI negative; however, the cells in the late stages of apoptosis were both annexin V and PI positive. The apoptotic index (%) was calculated as the sum of early and late apoptotic cells divided for the total number of events (Lee and Hong, 2010).

Western blot analysis
After treatment, cells were washed in 1× PBS and lysed in lysis buffer (10 mM Tris-HCl (pH 7.5), 10 mM NaH$_2$PO$_4$/NaHPO$_4$ (pH 7.5), 130 mM NaCl, 1% Triton X-100, 10 mM NaPPi, 1 mM phenylmethylsulfonyl fluoride, 2 μg/ml pepstatin A) for 30 min on ice. Lysates were centrifuged at 12,000 × g for 20 min at 4°C. The supernatant was collected, and the protein content of the supernatant was measured using a Bio-Rad protein assay kit (Bio-Rad Laboratories, USA) before analysis. The protein samples were loaded at 10 μg of protein/lane, separated by sodium dodecyl sulfate-polyacrylamide gel electrophoresis (SDS-PAGE) in 10-15% gel, and transferred to polyvinylidene difluoride membranes (Immun-Blot PVDF membrane, 0.2 μm; Bio-Rad). Membranes were blocked with 5% nonfat powered milk in 1× tris buffered saline containing 0.1% Tween 20 (TBS-T) for 1 h, and they were incubated with primary antibodies at 4°C overnight. Finally, the membranes were treated with HRP-linked secondary antibodies for 1 h at 4°C. The membranes were washed with TBS-T after each antibody binding reaction. Detection of each protein was performed using an enhanced
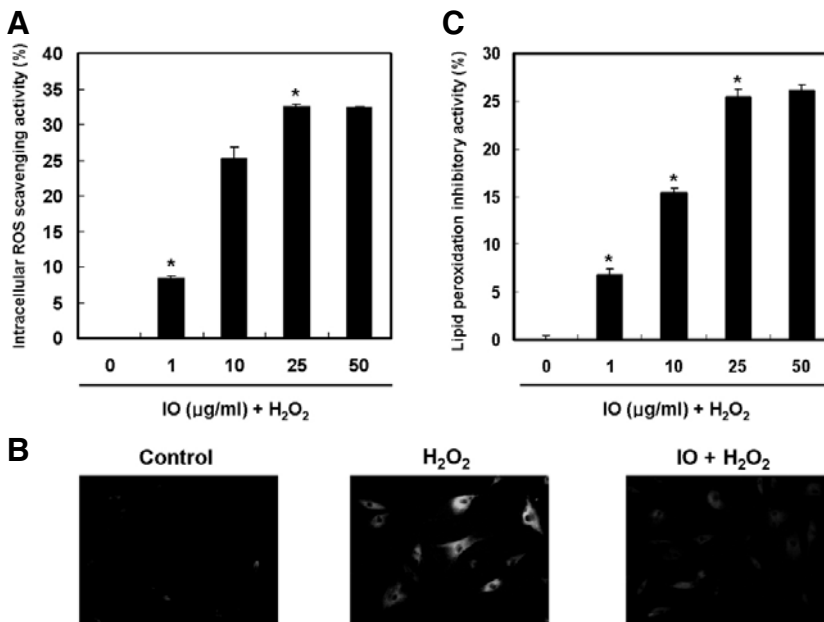
A

C

B

| Control | H₂O₂ | IO + H₂O₂ |

Fig. 1. Effect of *I. obliquus* on ROS scavenging and inhibition of lipid peroxidation. Confluent cells were incubated with *I. obliquus* extract for 4 h prior to exposure to 1 mM hydrogen peroxide for 2 h. (A) Intracellular ROS scavenging activity of *I. obliquus*. Intracellular ROS generation was detected using the DCF-DA method. (B) Fluorescence microscopic images of cells stained for ROS. Representative images illustrate the increased green fluorescence intensity of DCF produced by ROS in hydrogen peroxide-treated cells compared to control as well as the lowered fluorescence intensity in hydrogen peroxide-treated cells in the presence of *I. Obliquus* extract (25 μg/ml). Magnification: 400-fold. (C) Lipid peroxidation was detected by measuring the amount of TBARS. Data (A and C) represent the mean ± SE of three independent experiments. Significant differences were compared with the control at $*p < 0.05$ by Student's *t*-test.

che-miluminescence kit (Millipore Co., USA) (Lee and Hong, 2010).

Senescence-associated β-galactosidase staining

SA-β-gal staining was performed as previously described (Dimri et al., 1995). Briefly, cultured cells were washed in PBS, fixed with 3.7% paraformaldehyde for 15 min at room temperature, rinsed with PBS, and then incubated in freshly prepared SA-β-gal staining solution (1 mg/ml 5-bromo-4-chloro-3-indolyl β-D-galactoside, 5 mM potassium ferrocyanide, 5 mM potassium ferrocyanide, 2 mM magnesium chloride, pH 6.0) at 37°C overnight. At the end of the incubation, cells were washed with PBS. Senescent cells were identified as blue-stained cells by standard light microscopy at 100-fold magnification, and a total of 200 cells were counted in five random fields on a slide to determine the percentage of positively-stained cells.

Zymography analysis

SDS-PAGE substrate-embedded enzymography (zymography) analysis was used to identify enzymes activity with collagenase and gelatinase (Gibbs et al., 1999). Briefly, the supernatant collected from cell culture was resolved in 10% SDS-PAGE gels, which were prepared by the incorporation of gelatin (1 mg/ml) or β-casein (1 mg/ml) before casting. After electrophoresis, gels were washed twice for 30 min in 2.5% Triton X-100 with shaking. The gels were then incubated at 37°C for 24-48 h in reaction buffer containing 50 mM Tris-HCl (pH 7.6), 10 mM CaCl₂, 150 mM NaCl and 20% sodium azide, followed by staining with 0.25% Coomassie brilliant blue G-250 in 50% methanol and 10% acetic acid for 1-2 h. The completely stained gels were appropriately destained with 40% methanol and 10% acetic acid. The enzyme activities were evident as clear (unstained) regions against the dark background.

Collagen assay

Collagen content was determined using a Sircol collagen assay kit (Biocolor Ltd., UK) according to the manufacturer's instructions. This assay can assess the rate of newly synthesized collagen released into cell culture medium during cell growth and cell maintenance. Briefly, after various treatments, cultured

cells were lysed on ice in lysis buffer (50 mM Tris-HCl, pH 7.4, 150 mM NaCl, 1% NP-40, 0.25% sodium deoxycholate, 0.1% SDS, 1 mM phenylmethylsulphonyl fluoride, 1 mM pepstatin A) for 10 min on ice. Lysates were centrifuged at 12,000 × g for 20 min at 4°C after which the supernatant was collected and the protein content was measured using a Bio-Rad protein assay kit. Identical amounts of cell lysates were transferred to each tube along with 1 ml Sircol dye reagent. After shaking for 30 min, the precipitate was collected by centrifugation at 10,000 rpm for 10 min. One milliliter of the alkali reagent (0.5 M sodium hydroxide) for dissolution of the pellet was then added to each tube. After 10 min, the absorbance was measured spectrophotometrically at 540 nm.

In vivo experiments using mice

To induce skin wrinkles, a UV lamp with an emission spectrum between 280 and 360 nm (15 W, maximum wavelength 306 nm; BOGO UV Co. Ltd., Korea) was used. The irradiation intensity 30 cm from the light source was 1.0 mW/cm². The minimal erythma dose (MED) on mouse dorsal skin was measured. The dorsal skin of hairless mice was exposed to UV irradiation three times a week (Monday, Wednesday, and Friday). The irradiation dose was increased weekly by 1 MED increments (1 MED = 130 mJ/cm²) up to 4 MED, after which the irradiation was maintained at 4 MED until at 12 weeks. Female SKH-1 hairless mice were randomly divided into four groups of five mice each: the control group, UV-irradiated group, positive control group treated with retinol and the sample-treated group. To observe the effects of retinol and *I. obliquus* extracts on skin wrinkling formation, the positive control group was applied 0.5% retinol in vehicle (70% ethanol, 30% polyethylene glycol and 0.05% butylated hydroxytoluene). For the preparation of *I. obliquus* extracts (final concentration 1.0%), the extracts were mixed in vehicle (olive oil, 100% ethanol and distilled water). After irradiation with UV, completed samples were applied topically to the UV-exposed dorsal region of each mouse three times per week. To evaluate the formation of wrinkles after UV irradiation, each hairless mouse was anesthetized, after which the UV-exposed dorsal skin (wrinkle formation area) was photographed using a digital camera. For detailed morphological
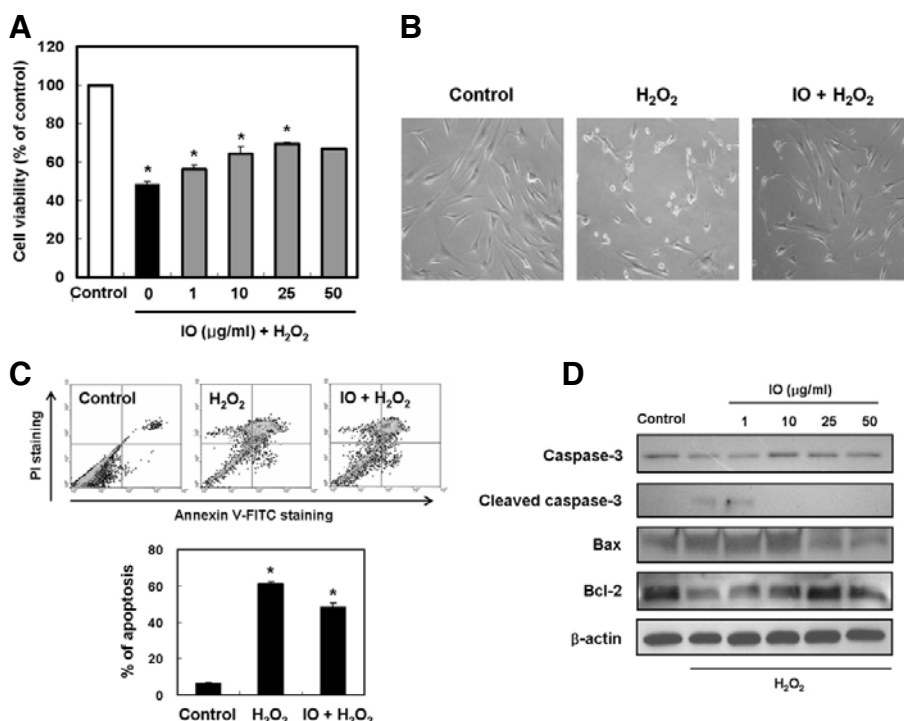
Fig. 2. Effect of *I. obliquus* on hydrogen peroxide-induced apoptosis in human dermal fibroblasts. (A) Protective effect of *I. obliquus* against oxidative damage induced by hydrogen peroxide was determined using the MTT assay. (B) Representative micrographs of hydrogen peroxide-induced morphological changes in cells treated with or without 1 mM hydrogen peroxide and 25 μg/ml *I. Obliquus* extract. Magnification: 100-fold. (C) The number of apoptotic cells was detected by the annexin V/PI flow cytometry analysis. The cells were treated with or without 25 μg/ml *I. obliquus* extract for 4 h prior to the addition of 1 mM hydrogen peroxide. Data (A and C) represent the mean $\pm$ SE of three independent experiments. Significant differences were compared with the control at *$p < 0.05$ by Student's *t*-test. (D) Altered expression of apoptotic-related proteins in cells treated with or without 25 μg/ml *I. obliquus* extract for 4 h prior to the addition of 1 mM hydrogen peroxide. The levels of caspase 3, Bax, and Bcl-2 were assessed using Western blot analysis. Equal loading of total proteins in each sample was verified by β-actin expression.

observation of wrinkles, skin impressions were photographed using a skin diagnosis system (AramHuvis Co., Korea). Skin fold thickness was measured every week using a caliper (Mitutoyo Co., Japan). Midline skin was manually pinched upward at the neck and at the base of the tail, and skin fold thickness was measured mid-way between the neck and hips.

Statistical analysis

Data were expressed as means $\pm$ standard errors (SEM), and the results were taken from at least three independent experiments performed in triplicate. The data were analyzed by Student's *t*-test to evaluate significant differences. A level of $p < 0.05$ was regarded as statistically significant.

RESULTS

Effect of *I. obliquus* on ROS scavenging and inhibition of lipid peroxidation

ROS levels in hydrogen peroxide-treated human dermal fibroblasts were determined using the ROS-sensitive fluorescent probe H$_2$DCFDA. The intracellular ROS scavenging activity of *I. obliquus* was 33% at a concentration of 25 μg/ml (Fig. 1A). In the fluorescent microscope images, the fluorescent intensity of the DCF-DA stain was enhanced in hydrogen peroxide-treated human dermal fibroblasts. However, *I. obliquus* reduced the green fluorescence intensity, which resulted from hydrogen peroxide treatment, indicating a reduction in ROS generation (Fig. 1B). In addition, the ability of *I. obliquus* to inhibit lipid peroxidation in hydrogen peroxide-treated human dermal fibroblasts was investigated. The generation of TBA reactive substance was inhibited in the presence of *I. obliquus*. The inhibitory effect of *I. obliquus* was 26% at 25 μg/ml compared to 7% inhibition in the untreated group (Fig. 1C). Overall, the results indicated that endogenous antioxidants of *I. obliquus* might be

useful in preventing oxidative damage caused by ROS.

Effect of *I. obliquus* on hydrogen peroxide-induced apoptosis in human dermal fibroblasts

The protective effect of *I. obliquus* on cell survival in hydrogen peroxide-treated human dermal fibroblasts was measured using a MTT assay. The cells were pretreated with *I. obliquus* at various concentrations (from 1 to 50 μg/ml) for 4 h, followed by treatment with 1 mM hydrogen peroxide treatment for 2 h. In these experiments, the cell viability of control decreased to 48.4% after hydrogen peroxide treatment. Treatment with *I. obliquus* restored the cell viability back up to 69.5% at a concentration of 25 μg/ml (Fig. 2A). To further confirm the protective effect of *I. obliquus* on cell survival in hydrogen peroxide-treated cells, we performed a morphology study. Cells in dishes supplemented with 1 mM hydrogen peroxide became sparse, rounded and detached from the dishes. However, these abnormal morphological changes were inhibited in the presence of *I. obliquus* (Fig. 2B). To evaluate whether or not the growth-inhibitory effect of hydrogen peroxide was associated with apoptosis, a double-staining method using FITC-labeled annexin V and PI was performed. Double staining the cells with annexin V and PI allowed us to detect apoptotic cells by flow cytometry. Treatment with 1 mM hydrogen peroxide caused 61.3% of the cells to undergo apoptosis. However, pretreatment with *I. obliquus* markedly inhibited hydrogen peroxide-induced apoptotic cell death (Fig. 2C). To study the mechanism by which *I. obliquus* mediates the inhibition of apoptosis, the effects of pretreatment with *I. obliquus* on the altered expression of apoptotic-related proteins in hydrogen peroxide-treated human dermal fibroblasts were analyzed by Western blot analysis. Compared to controls, caspase 3 was activated after hydrogen peroxide treatment. Moreover, the pro-apoptotic protein Bax was increased in expression while the anti-apoptotic
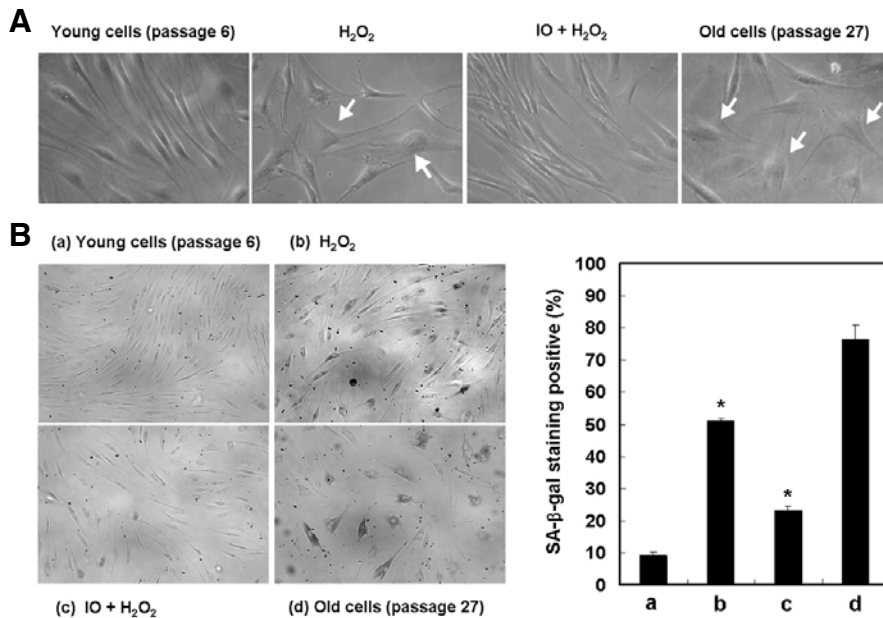
Fig. 3. Effect of *I. obliquus* on hydrogen peroxide-induced premature senescence in human dermal fibroblasts. The cells were treated with 500 μM hydrogen peroxide for 2 h in the presence or absence of *I. obliquus* extract (25 μg/ml) and then recovered for 7 days with fresh medium. (A) Morphological observation of cells was detected by optical microscopy. Magnification: 200-fold. Arrows indicate changed morphology, such as flattened and irregular cell morphology or enlarged cell size according to premature senescence. (B) Representative micrographs of young cells (passage 6), 500 μM hydrogen peroxide-induced premature senescent cells, *I. obliquus*-treated cells, and old cells (passage 27) after SA-β-gal staining. Magnification: 100-fold. The percentage of SA-β-gal positively stained cells was quantified as described in Section 2. Data represents the mean ± SE of three independent experiments. Significant differences were compared with the control at *$p <$ 0.05 by Student's *t*-test.

protein Bcl-2 was downregulated after hydrogen peroxide treatment. These results demonstrated that mitochondria-mediated apoptotic pathways were involved in hydrogen peroxide-induced apoptosis in human dermal fibroblasts. In comparison, pro-caspase 3 cleavage was remarkably inhibited in response to pretreatment with *I. obliquus*. Additionally, pretreatment with *I. obliquus* decreased expression of the pro-apoptotic protein Bax and increased expression of the anti-apoptotic protein Bcl-2 in hydrogen peroxide-treated human dermal fibroblasts (Fig. 2D). These findings indicated that *I. obliquus* exhibited protective effects against oxidative stress-induced apoptosis in human dermal fibroblasts.

Effect of *I. obliquus* on hydrogen peroxide-induced premature senescence in human dermal fibroblasts
To investigate the effect of *I. obliquus* on hydrogen peroxide-induced senescence in human dermal fibroblasts, we first induced premature fibroblasts senescence by the addition of 500 μM hydrogen peroxide for 2 h. We found that treatment with *I. obliquus* inhibited the senescent phenotype as judged by SA-β-gal assay and an enlarged and flattened cell morphological appearance. After treatment with hydrogen peroxide, 51.1% of cells were SA-β-gal positive, compared to only 23.2% of *I. obliquus* (50 μg/ml)-treated cells (Fig. 3). These results indicated that *I. obliquus* exerted protective effects against oxidative stress-induced premature senescence in human dermal fibroblasts.

Effect of *I. obliquus* on hydrogen peroxide-induced MMP activity and collagen degradation in human dermal fibroblasts
Matrix metalloproteinases (MMPs) play a prominent role in the breakdown of connective tissue components such as collagen, a major dermal extracellular matrix during cellular senescence. Therefore, the effect of *I. obliquus* on hydrogen peroxide-induced MMPs activity and collagen synthesis in human dermal fibroblasts was investigated. The zymogrphy data revealed that hydrogen peroxide elevated the enzyme activities of MMP-1

and MMP-9, but not MMP-2. However, treatment with *I. obliquus* inhibited the increased activities of MMP-1 and MMP-9 in a dose-dependent manner (Fig. 4A). Conversely, related to the inhibitory effect on MMPs, *I. obliquus* significantly reversed the decreased expression of collagen in a dose-dependent manner (Fig. 4B). These results suggested that *I. obliquus* increased collagen synthesis through inhibition of MMPs activity in hydrogen peroxide-treated human dermal fibroblasts.

Effect of *I. obliquus* on UV irradiation-induced wrinkle formation and skin thickening in hairless mice
To investigate the effects of *I. obliquus* on UV-induced skin changes, including skin thickening and wrinkle formation, the dorsal skins of hairless mice were exposed to UV with or without topical treatment with *I. obliquus* for 12 weeks. The repetitive exposure of hairless mice to UV radiation increased skin thickness and wrinkle formation. However, topical treatment with retinol or *I. obliquus* remarkably reduced UV-induced skin thickening and wrinkle formation (Fig. 5). These results showed that *I. obliquus* could suppress UV-induced skin thickening and wrinkle formation.

DISCUSSION

Chronic exposure of the skin to UV radiation is known to induce various harmful effects, including skin thickening, wrinkle formation, inflammation and carcinogenesis. It has been shown that UV irradiation leads to excessive generation of ROS, thereby resulting in an oxidative stress state (Ibbotson et al., 1999; Scharffetter-Kochanek et al., 1997). Therefore, it is likely that ROS generated by UV irradiation play a critical role in UV-induced skin damage. Accordingly, it has been shown that inhibition of ROS production and/or enhancement of ROS scavenging can be used as beneficial therapies for the treatment of UV-induced skin damage (Harman, 1956). Antioxidants have the capacity to quench ROS, and therefore are an example of a compound that can be used for this purpose (Diplock et al., 1998). Although some synthetic antioxidants, such as butylated
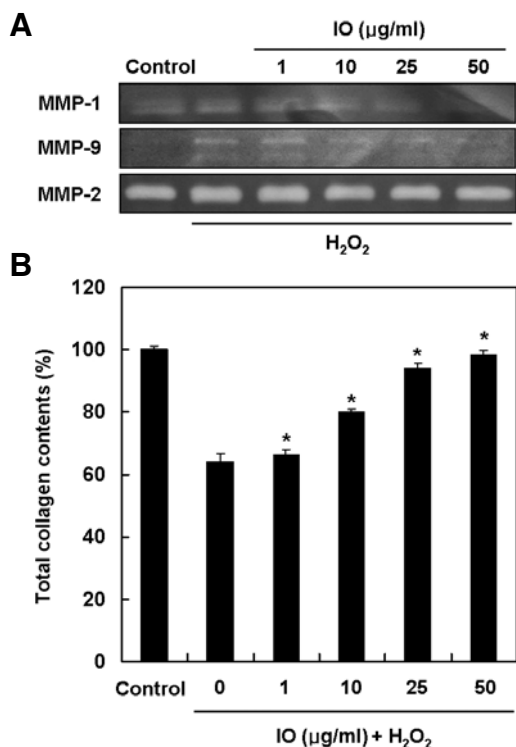
A

B

Fig. 4. Effect of *I. obliquus* on hydrogen peroxide-induced MMP activity and collagen degradation in human dermal fibroblasts. (A) The cells were treated with 1 mM hydrogen peroxide for 2 h in the presence or absence of *I. obliquus* extract and collected supernatant after recovered with serum-free DMEM for 48 h. The caseinolytic activity MMP-1 and the gelatinolytic activities of MMP-2 and MMP-9 were determined by casein- and gelatin-zymography, respectively. (B) The cells were treated with 1mM hydrogen peroxide for 2 h in the presence or absence of *I. obliquus* extract and then harvested further incubation with serum-free DMEM for 48 h. Total cell lysates were measured for their total collagen contents using a Sircol assay kit. Data represents the mean ± SE of three independent experiments. Significant differences were compared with the control at *$p < 0.05$ by Student's *t*-test.

A

B

Fig. 5. Effect of *I. obliquus* on UV irradiation-induced wrinkle formation and skin thickening in hairless mice. UV irradiation exposed three times a week for 12 weeks in the back skins of hairless mice. After UV exposure, retinol (0.5%), vehicle alone or *I. obliquus* extract (1.0%) were applied. (A) Photodamaged dorsal skin (wrinkle formation area) was photographed by a skin diagnosis system. Magnification: 10-fold or 60-fold. (B) Skin thickness was measured midway between the neck and hips with a caliper every week. Data represents the mean ± SE of three independent experiments. Significant differences were compared with the UV control at *$p < 0.05$ by Student's *t*-test.

hydroxyanisole (BHA) and butylated hydroxytoluene (BHT), exhibit antioxidant effects against free radicals, various studies have shown that they also possess toxicological effects compared to natural antioxidants. Thus, there has been a gradual increase in the demand for alternative and safe antioxidants isolated from natural sources (Saito et al., 2003). Although some reports have suggested that *I. obliquus* exhibits potent free radical scavenging effects (Lee et al., 2007; Park et al., 2004), there have been no reports on the preventive effects of *I. obliquus* treatment on oxidative stress-induced apoptosis and premature senescence.

Many studies have demonstrated the cytotoxic effects of oxidizing agents such as hydrogen peroxide on human fibroblasts (Chen, 2000; Ohshima, 2004; Rhee, 2006). In response to hydrogen peroxide, pro-apoptotic Bcl-2 family proteins such as Bax initiate the mitochondria-mediated apoptotic pathway by forming channels on assimilating into the mitochondria, thus increasing outer mitochondria membrane permeability, and thereby facilitating the release of cytochrome c and other pro-apoptotic factors from the mitochondrial intermembrane space. Released cytochrome c forms an apoptosome complex with
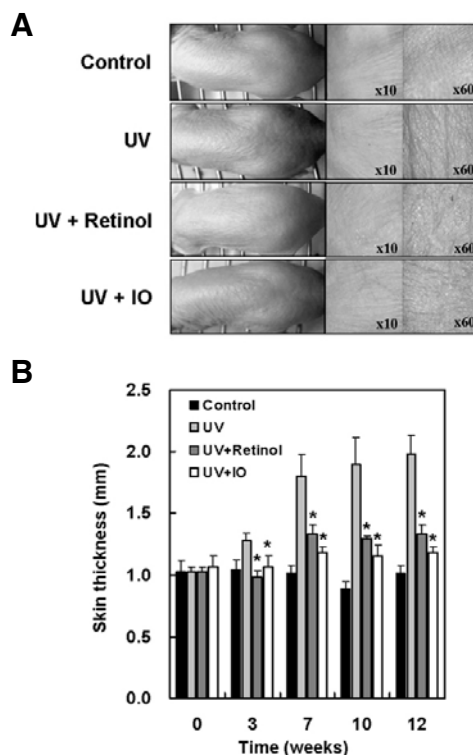
Apaf-1, which activates caspase 9, and in turn, its downstream caspase 3, resulting in the morphological features of apoptosis (Cohen, 1997; Yuan et al., 2003). In agreement with this, cells exposed to hydrogen peroxide exhibited an increased number of apoptotic fibroblasts as demonstrated by exposure of phosphatidylserine, a reduced ratio of Bcl-2/Bax protein expression, and increased caspase 3 activity. However, cells that were pretreated with *I. obliquus* resulted in a reduced percentage of apoptotic cells (Fig. 2). These results indicate that the inhibition of intracellular ROS generation and lipid peroxidation may be important for cytoprotection against oxidative damage (Fig. 1). Therefore, these results suggest that *I. obliquus* inhibited oxidative stress-induced apoptosis through its ROS scavenging effects in human dermal fibroblasts.

Oxidative stress has been shown to induce stress-induced premature senescence in fibroblasts (Dasari et al., 2006; Frippiat et al., 2001). Senescent cells show different features from proliferative cells. A typical senescence-specific morphology is characterized as 'flattened and enlarged' cells (Hayflick and Moorhead, 1961). SA-β-gal activity is commonly used as a senescent marker. Since this enzyme works under acidic pH conditions in a senescence-specific manner, the positive cells in this assay recognized as senescent cells (Dimri et al., 1995). In the same manner, cells treated with hydrogen peroxide exhib-

ited the senescent phenotype as judged by SA-β-gal assay as well as an enlarged and flattened cell morphological appearance. However, cells that were pretreated with *I. obliquus* experienced a reduction in the number of senescent cells (Fig. 3). ROS such as hydrogen peroxide increase MMP secretion in human dermal fibroblasts (Brenneisen et al., 1997). *I. obliquus* increased collagen synthesis through inhibition of MMP-1 and MMP-9 in hydrogen peroxide-treated human fibroblasts (Fig. 4). In addition, *I. obliquus* suppressed UV-induced morphologic skin changes, such as skin thickening and wrinkle formation, in hairless mice *in vivo* (Fig. 5). Therefore, these results suggest that *I. obliquus* inhibited oxidative stress-induced premature senescence through its ROS scavenging effects.

In conclusion, *I. obliquus* exerted ROS scavenging activity, inhibited hydrogen peroxide-induced apoptosis, and inhibited hydrogen peroxide or UV-induced premature senescence.

REFERENCES

Brenneisen, P., Briviba, K., Wlaschek, M., Wenk, J., and Scharffetter-Kochanek, K. (1997). Hydrogen peroxide (H_2O_2) increases the steady-state mRNA levels of collagenase/MMP-1 in human dermal fibroblasts. Free Radic. Biol. Med. *22*, 515-524.

Chen, Q.M. (2000). Replicative senescence and oxidant-induced premature senescence. Beyond the control of cell cycle checkpoints. Ann. N Y Acad. Sci. *908*, 111-125.

Cohen, G.M. (1997). Caspases: the executioners of apoptosis. Biochem. J. *326*, 1-16.

Dasari, A., Bartholomew, J.N., Volonte, D., and Galbiati, F. (2006). Oxidative stress induces premature senescence by stimulating caveolin-1 gene transcription through p38 mitogen-activated protein kinase/Sp1-mediated activation of two GC-rich promoter elements. Cancer Res. *66*, 10805-10814.

Dimri, G.P., Lee, X., Basile, G., Acosta, M., Scott, G., Roskelley, C., Medrano, E.E., Linskens, M., Rubelj, I., Pereira-Smith, O., et al. (1995). A biomarker that identifies senescent human cells in culture and in aging skin *in vivo*. Proc. Natl. Acad. Sci. USA *92*, 9363-9367.

Diplock, A.T., Charleux, J.L., Crfozier-Willi, G., Kok, F.J., Rice-Evans, C., Roberfroid, M., Stahl, W., and Vina-Ribes, J. (1998). Functional food science and defence against reactive oxidative species. Br. J. Nutr. *80*, 77-112.

Frippiat, C., Chen, Q.M., Zdanov, S., Magalhaes, J.P., Remacle, J., and Toussaint, O. (2001). Subcytotoxic H_2O_2 stress triggers a release of transforming growth factor-β1, which induces biomarkers of cellular senescence of human diploid fibroblasts. J. Biol. Chem. *276*, 2531-2537.

Gibbs, D.F., Warner, R.L., Weiss, S.J., Johnson, K.J., and Varani, J. (1999). Characterization of matrix metalloproteinases produced by rat alveolar macrophages. Am. J. Respir. Cell Mol. Biol. *20*, 1136-1144.

Harman, D. (1956). Aging: a theory based on free radical and radiation chemistry. J. Gerontol. *11*, 298-300.

Hayflick, L., and Moorhead, P.S. (1961). The serial cultivation of human diploid cell strains. Exp. Cell Res. *25*, 585-621.

Ibbotson, S.H., Moran, M.N., Nash, J.F., and Kochevar, I.E. (1999). The effects of radicals compared with UVB as initiating species for the induction of chronic cutaneous photodamage. J. Invest. Dermatol. *112*, 933-938.

Jang, J.S., Lee, J.S., Lee, J.H., Kwon, D.S., Lee, K.E., Lee, S.Y., and Hong, E.K. (2010). Hispidin produced from *Phellinus linteus* protects pancreatic β-cells from damage by hydrogen peroxide. Arch. Pharm. Res. *33*, 853-861.

Jeong, J.B., Park, J.H., Lee, H.K., Ju, S.Y., Hong, S.C., Lee, J.R., Chung, G.Y., Lim, J.H., and Jeong, H.J. (2009). Protective effect of the extracts from *Cnidium officinale* against oxidative damage

induced by hydrogen peroxide via antioxidant effect. Food Chem. Toxicol. *47*, 525-529.

Kim, Y.O., Park, H.W., Kim, J.H., Lee, J.Y., Moon, S.H., and Shin, C.S. (2006). Anti-cancer effect and structural characterization of endo-polysaccharide from cultivated mycelia of *Inonotus obliquus*. Life Sci. *79*, 72-80.

Kim, H.G., Yoon, D.H., Kim, C.H., Shrestha, B., Chang, W.C., Lim, S.Y., Lee, W.H., Han, S.G., Lee, J.O., Lim, M.H., et al. (2007). Ethanol extract of *Inonotus obliquus* inhibits lipopolysaccharide-induced inflammation in RAW 264.7 macrophage cells. J. Med. Food *10*, 80-89.

Lee, J.S., and Hong, E.K. (2010). *Hericium erinaceus* enhances doxorubicin-induced apoptosis in human hepatocellular carcinoma cells. Cancer Lett. *297*, 144-154.

Lee, I.K., Kim, Y.S., Jang, Y.W., Jung, J.Y., and Yun, B.S. (2007). New antioxidant polyphenols from the medicinal mushroom *Inonotus obliquus*. Bioorg. Med. Chem. Lett. *17*, 6678-6681.

Lee, J.S., Cho, J.Y., and Hong, E.K. (2009). Study on macrophage activation and structural characteristics of purified polysaccharides from the liquid culture broth of *Hericium erinaceus*. Carbohydr. Polym. *78*, 162-168.

Nakajima, Y., Nishida, H., Nakamura, Y., and Konishi, T. (2009). Prevention of hydrogen peroxide-induced oxidative stress in PC12 cells by 3,4-dihydroxybenzalacetone isolated from Chaga (*Inonotus obliquus* (persoon) Pilat). Free Radic. Biol. Med. *47*, 1154-1161.

Nobel, C.I., Kimland, M., Lind, B., Orrenius, S., and Slater, A.F. (1995). Dithiocarbamates induce apoptosis in thymocytes by raising the intracellular level of redox active copper. J. Biol. Chem. *270*, 26202-26208.

Ohshima, S. (2004). Apoptosis in stress-induced and spontaneously senescent human fibroblasts. Biochem. Biophys. Res. Commun. *324*, 241-246.

Park, Y.K., Lee, H.B., Jeon, E.J., Jung, H.S., and Kang, M.H. (2004). Chaga mushroom extract inhibits oxidative DNA damage in human lymphocytes as assessed by comet assay. BioFactors *21*, 109-112.

Rhee, S.G. (2006). Cell signaling. H_2O_2, a necessary evil for cell signaling. Science *312*, 1882-1883.

Saito, M., Sakagami, H., and Fujisawa, S. (2003). Cytotoxicity and apoptosis induction by butylated hydroxyanisole (BHA) and butylated hydroxytoluene (BHT). Anticancer Res. *23*, 4693-4701.

Saraste, A., and Pulkki, K. (2000). Morphologic and biochemical hallmarks of apoptosis. Cardiovasc. Res. *45*, 528-537.

Scharffetter-Kochanek, K., Wlaschek, M., Brenneisen, P., Schauen, M., Blaudschun, R., and Wenk, J. (1997). UV-induced reactive oxygen species in photocarcinogenesis and photoaging. Biol. Chem. *378*, 1247-1257.

Schindowski, K., Leutner, S., Kressmann, S., Eckert, A., and Muller, W.E. (2001). Age-related increase of oxidative stress-induced apoptosis in mice prevention by Ginkgo biloba extract (EGb761). J. Neural Transm. *108*, 969-978.

Scorrano, L. (2009). Opening the doors to cytochrome c: changes in mitochondrial shape and apoptosis. Int. J. Biochem. Cell Biol. *41*, 1875-1883.

Serrano, M., and Blasco, M.A. (2001). Putting the stress on senescence. Curr. Opin. Cell Biol. *13*, 748-753.

Touissant, O., Dumont, P., Dierick, J.F., Pascal, T., Frippiat, C., Chainiaux, F., Sluse, F., Eliaers, F., and Remacle, J. (2000). Stress-induced premature senescence. Ann. N Y Acad. Sci. *908*, 85-98.

Yu, J.Y., Kim, J.H., Kim, T.G., Kim, B.T., Jang, Y.S., and Lee, J.C. (2010) (E)-1-(3,4-dihydroxyphenethyl)-3-styrylurea inhibits proliferation of MCF-7 cells through G1 cell cycle arrest and mitochondria-mediated apoptosis. Mol. Cells *30*, 303-310.

Yuan, J., Murrell, G.A., Trickett, A., and Wang, M.X. (2003). Involvement of cytochrome c release and caspase-3 activation in the oxidative stress-induced apoptosis in human tendon fibroblasts. Biochim. Biophys. Acta *1641*, 35-41.